Interner Bericht
DESY D3-74
March 1993

Attenuation of the neutron dose equivalent in labyrinths through an accelerator shield.

H. Dinter, D. Dworak* and K. Tesch.

Deutsches Elektronen-Synchrotron DESY,
Notkestr. 85, D-2000 Hamburg 52, Germany

Abstract: The attenuation of the neutron dose equivalent in labyrinths is calculated. Long straight access ways and rectangular 3-sectional labyrinths are considered. The Monte Carlo calculations are checked against earlier measurements. Simple formulas for the relative attenuation in the second and in the third section are derived. Absolute values of neutron doses are given for several cases of beam losses near the mouth of a labyrinth at proton accelerators. Associated photon doses are also calculated.

To be published

*On leave of absence from the Institute of Nuclear Physics, Krakow, Poland.

1. Introduction

There are two main shielding problems at accelerators, the attenuation of scattered radiation through bulk shielding, and the attenuation along access ways leading through the shield. The first-mentioned problem is the object of numerous articles. The most recent shielding calculations can be found in ref. 1–3, and good reviews of earlier calculations and measurements are available (4, 5). On the contrary, the literature covering the second problem is scarce. The attenuation of the neutron dose equivalent in labyrinths were studied by Tesch (6) ten years ago both with isotopic neutron sources and at electron accelerators. The resulting attenuation functions were more or less confirmed by measurements of Ban et al. (7) and Belogorlov et al. (8) with neutron sources, and by calculations of Kryuchkov (9) using the code MOSKIT and an AmBe spectrum. At a high energy proton accelerator these functions were measured by Cossairt et al. (10). Some other papers are mentioned in the review article (4). Most of these works suffer from certain deficiencies. The measurements (6, 7) were performed with rem-counters after Andersson and Braun, these instruments underestimate the dose equivalent of thermal neutrons which is important in the second and third section of a labyrinth as we will show below. Cossairt et al. measured the absorbed dose instead of dose equivalent. Earlier calculations use older codes so that especially a new calculation of the source term (i.e. the dose equivalent at the mouth of the labyrinth) is desirable.

Our calculations will cover the following items: a) Checking the Monte Carlo code used to calculate neutron transport against measurements performed with isotopic neutron sources. b) Calculating the source term at proton accelerators with a mod-

ern code, including the dependence on energy and target thickness.

c) Accurate calculation of the relative attenuation of the neutron dose equivalent in a long first section and in the second and third section of rectangular labyrinths, especially considering the dependence on the cross section of the labyrinth.

d) Calculation of the dose of photons produced by neutrons in the concrete walls.

2. Codes, neutron sources, and detectors

The well-known Monte Carlo code MORSE-CG was used to calculate the neutron transport in a labyrinth. The actual version was taken from the HERMES code system (11). Only two non-analog features of the code were used: the weight of a particle is reduced by the absorption probability at each collision, and Russian roulette is played each time when the weight drops below 0.1 to reduce the particle population. The HERMES combinatorial geometry module gives the possibility to define semi-infinite bodies of which the walls of rectangular concrete labyrinths are constructed. The use of the semi-infinite bodies helps to avoid numerical problems in the course of calculations. The HILO86 package (12) was used as input data, which is a multigroup library of 66 neutron groups covering the energy range from thermal energy up to 400 MeV, coupled with 22 photon groups from 10 keV to 20 MeV; it is based on the compilation ENDF/B-V. The history of a neutron is terminated if it escapes from the system or if it is killed by Russian Roulette.

We used the spectrum of an AmBe neutron source published by Kluge and Weise (13) for our comparisons with measurements, it was subdivided according to the HILO group structure. The source was placed inside a concrete house (the "accelerator room") opposite to the mouth of the labyrinth. At the beginning we calculated

the attenuation in a one-step-calculation using standard MORSE subroutines. To improve statistics, most of our calculations were performed in 2 steps. In a first step a plane source was determined covering the mouth of the labyrinth with a neutron distribution in energy and two angles which includes neutrons backscattered from the concrete house in addition to the neutrons from the point source. Both parts are of similar magnitude as it was already mentioned in ref. 6. In a second step the attenuation of the dose equivalent in a labyrinth was calculated relative to the dose equivalent of the plane source.

All neutron fields produced by a proton beam were calculated in two steps. The plane source at the beginning of each labyrinth was calculated by means of the Monte Carlo code FLUKA developed at CERN (14) and extended to low neutron energies (1). A comprehensive and improved version will soon be officially released by the CERN authors, it gives practically the same results (15) if applied in fields like shielding and dosimetry.

Measurements of neutron dose equivalent in labyrinths were done and will be done with instruments which are approximately sphere-like. We decided to choose the neutron fluence (number of neutrons per unit area, divided by the cosines of their angles between flight direction and normal of boundary) as the magnitude of interest. It is multiplied by fluence-to-dose conversion factors which we took from the same compilation (16) as in our earlier papers. We calculated the fluence in several ways as a check of scoring methods. Using the boundary crossing estimator neutrons were counted which cross plane detectors with an area equal to the cross section of the labyrinth, as well as neutrons crossing spherical detectors with diameter 50 cm.

The track length estimator was used to calculate neutron tracklengths inside 50 cm spheres. The results were in agreement, so we used the plane detector in most cases since it gives the best statistical accuracy.

3. Attenuation of doses from an AmBe neutron source

An AmBe source was positioned in a concrete house and the attenuation of neutron dose equivalent along labyrinths was calculated for comparison with measurements. Several 2- and 3-sectional labyrinths with different cross sections were chosen in order to check the MORSE code applied to this problem. Fig. 1 shows an example. The measurements and a derived attenuation formula are taken from Tesch (6), another relationship also based on measurements is from Ban et al. (7). The compositions of the concrete types can be found in ref. 1. All results are normalized to each other at $r_2 = 0$. The MORSE calculations show good agreement with measurements except for $r_2 > 5$ m. We found the same behaviour in a 3-sectional labyrinth (its geometry is shown in fig. 5 of ref. 6) where increasing deviations show up for $r_3 > 3$ m. The reason is the contribution of thermal neutrons to the dose equivalent which increase with distance in the second and further sections and for which the used rem-meters have an inadequate response. The discrepancies nearly disappear if the calculations are corrected for the known response of the instrument. We conclude that the MORSE code is a suitable instrument to calculate neutron doses in labyrinths.

4. Attenuation of neutron doses in labyrinths at proton accelerators

4.1. The source term

A proton beam in a cylindrical concrete tunnel is assumed to hit a long iron target near the mouth of a labyrinth. The produced dose per proton depends on beam energy, target dimension (especially its thickness), position of target relative to the labyrinth, and on the tunnel geometry because of backscattering. We first determined that target position which gives a maximum dose at the entrance. The resulting geometry was kept unchanged in all following calculations and is show in fig. 2. We calculated the neutron distribution of the plane source 2.5 x 3 m^2 as the first part of our two-step-calculation (see section 2) and studied the dose equivalent averaged over this area as a function of beam energy and target thickness.

The total dose equivalent H per proton averaged over the area indicated in fig. 2 and with a target diameter of 4 cm can be expressed as a function of beam energy

$$H = 2.3 \cdot 10^{-15} E_p^{0.83} \qquad (1)$$

$$H(Sv), E_p(GeV)$$

which we checked in the E_p range 10–1000 GeV. This is the known $E_p^{0.8}$ dependence of H behind shieldings, its reason is explained in ref. 2.

The dependence on target diameter is given in tab. 1 at $E_p = 100$ GeV. The neutron fluence spectrum at this energy and target diameter 4 cm is shown in fig. 3, it is

the douple-peak distribution of evaporation neutrons and spallation neutrons found experimentally and theoretically behind concrete shields (17). The ratio of the two peaks naturally depends on the target thickness and is also given in tab. 1. The spectrum depends on the relative position of scoring area and target, fig. 3 refers strictly to the geometry of fig. 2. It was found to be independent of the beam energy in the range 10–1000 GeV, which is not surprising considering the relatively low neutron energies emitted from the target at angles around 90°.

4.2 Attenuation in the first section

We studied the attenuation of neutron dose equivalent from the plane source described in the preceding section along the first section of a labyrinth (i.e. in a straight access way). The walls of all labyrinths are composed of ordinary concrete, floors and roofs are 100 cm thick. First we used a beam energy of 100 GeV. The target thickness is always 4 cm. The relative attenuation curves are shown in fig. 4 for 4 labyrinths with different cross sections A. They are well approximated by the equation

$$H(r_1)/H_0 = 0.98\, e^{-0.80 r_1/\sqrt{A}} + 0.02 \qquad (2)$$

in the region $r_1/\sqrt{A} < 7$. For r_1 >10 m the curves are a simple $1/r_1^2$ dependence, i.e. $H(r_1) = H(10)(12/(2 + r_1))^2$ for our geometry of fig. 2. This dependence holds for distances up to 75 m which we checked in case of an acces way with a 4 x 4 m^2 cross section. For small r_1 values the dependence of H on r_1 is more complicated since the target does not present a point source and the neutrons scattered back from the concrete house also contribute. Eq. 2 agrees with a curve published in

ref. 4, fig. A11, labelled "point source".

The spectrum of our plane source (fig. 3) remains unchanged along the section except that the contribution of high energy neutrons around 100 MeV is reduced on the first few meters and a peak of thermal neutrons appears, but the contribution of thermal neutrons to the dose equivalent is still negligible in the first section. Since the spectrum of the source does not depend on beam energy in the range 10–1000 GeV (see section 4.1), the relative attenuation curves for different primary energies are exactly the same.

4.3. Attenuation in the second section

The attenuation in the second (and in the third) section was calculated only for one primary energy (100 GeV) since it is independent of that magnitude. The curves are shown in fig. 5, upper right part, for 5 labyrinths. All sections of each labyrinth have the same cross section A. The steep and nearly exponential decrease at the beginning is due to the "disappearance" of the source and of the scattering material near the source, while a much smaller exponential term can describe the slow attenuation of neutrons scattered near the mouth of the second section into this section. The curves approximately collapse into one curve if r_2 is substituted by r_2/A^c. A best fit results with $c = 0.5$ or 0.55, so we choose again the $r_2/\sqrt{A}$ dependence which is shown in fig. 5, lower left part. This curve is well discribed by

$$H(r_2)/H_0 = 0.74\,e^{-10\,r_2/\sqrt{A}} + 0.21\,e^{-1.6\,r_2/\sqrt{A}} + 0.05\,e^{-0.54\,r_2/\sqrt{A}} \qquad (3)$$

Also shown are the corresponding curve of ref. 6 and the curve of Goebel et al. (ref. 4,

fig. A13). A quite good agreement is shown though our present calculations give a slower decrease for large r_2.

The neutron dose equivalent spectrum is presented in fig. 6 at $r_2 = 6$ m and is compared with the spectrum received when substituting the plane source by an AmBe source. Though it is difficult to achieve good statistical accuracy the figure demonstrates the close similarity of both spectra. This explains the fact that attenuation in labyrinths at accelerators can well be studied by isotopic neutron sources.

4.4. Attenuation in the third section

The dose equivalent attenuation was calculated in 4 labyrinths with a third section and with A between 3 x 3 m^2 and 2.2 x 1 m^2. The curves approximately coincide if again plotted as a function of $r_3/\sqrt{A}$. This function is well fitted by

$$H(r_3)/H_0 = 0.81\, e^{-3.8\, r_3/\sqrt{A}} + 0.19\, e^{-0.70\, r_3/\sqrt{A}} \qquad (4)$$

and is displayed in fig. 7. Also shown is the corresponding curve of the second section, a clear difference is seen. The reason is the change in the neutron spectrum, viz. the increasing contribution of thermal neutrons to the dose equivalent. Whereas their contribution in the second section is between 20% (for $A = 4$ x 4 m^2) and 35% ($A = 2$ x 1.5 m^2), it amounts to 60% (for $A = 2$ x 1.5 m^2) in the third sections. Thermal neutrons are scattered more easily around a rectangular bend. This can be demonstrated by substituting the plane source at the mouth of the labyrinth by a source of thermal neutrons with isotropic angular distribution, their attenuation

curve is also entered into fig. 7.

The difference in dose equivalent attenuation between the two sections were not found experimentally in ref. 6 because of the reduced sensitivity of the used instrument to thermal neutrons.

5. Photon doses

Photon doses are expected in labyrinths due to inelastic scattering of neutrons and capture of thermal neutrons in the concrete walls. This contribution can also be calculated since data on photoproduction are available in the HILO library, and the produced photons are transported by the standard MORSE code. Photons produced in the target by the proton beam were not considered; photon doses produced in an accelerator tunnel and attenuated within a labyrinth were studied in ref. 18.

The results of our present investigation can be summarized as follows. The ratio of photon dose to neutron dose equivalent is smaller than 1% in the first section of a labyrinth and around 5% in the second section, in the third section it is (8±2)%. The latter number is the same ratio we found for nuclear photons behind bulk concrete shields around proton accelerators (3).

6. Concluding remarks

In the present paper we stated the similarity of neutron spectra in the second section of a labyrinth produced either by an AmBe source or by absorption of high energy protons. In ref. 6 we found the same attenuation functions with an AmBe neutron source and at electron accelerators. We conclude that eqs. 3 and 4 decribing the

relative attenuation of neutron dose equivalent in the second and third section of a concrete labyrinth are valid at all accelerators with energies high enough to produce neutrons with energies of a few MeV. The absolute values of doses along labyrinths at high energy proton accelerators can be calculated by means of eqs. 1 to 4 and tab. 1 if one of the configurations described in section 4.1 can be assumed as a possible beam loss geometry.

References

(1) J.M. Zazula and K. Tesch, Nucl. Instr. and Meth. A286 (1990) 279.

(2) K. Tesch and J.M. Zazula, Nucl. Instr. and Meth. A300 (1991) 179.

(3) D. Dworak, K. Tesch and J.M. Zazula, Nucl. Instr. and Meth. A321 (1992) 589.

(4) A. Fasso, K. Goebel, M. Höfert, J. Ranft and G. Stevenson, Landolt-Börnstein, New Series, Group I Vol. 11, Springer Verlag Berlin 1990.

(5) R.H. Thomas and G.R. Stevenson, IAEA Technical Report Series No. 283, Vienna 1988.

(6) K. Tesch, Part. Accelerators 12 (1982) 169.

(7) S. Ban and H. Hirayama, Proc. 5. Symp. Accelerator Science and Technology, Tsukuba, Japan, 1984.

(8) E.A. Belogorlov, G.I. Britvich, V.B. Getmanov, A.I. Dronov, A.A. Kuznetsov, G.I. Krupnyi, V.N. Lebedev, V.S. Lukanin, V.N. Peleshko, Ya.N. Rastsvetalov, Serpukhov Inst. High Energy Physics, IFVE85-4 (1985).

(9) V. Krjuchkov, Inst. High Energy Physics, Protvino, Russia, 1992 (private communication).

(10) J.D. Cossairt, J.G. Couch, A.J. Elwyn and W.S. Freeman, Health Physics 49 (1885) 907.

(11) P. Cloth, D. Filges, R.D. Neef, G. Sterzenbach, Ch. Reul, T.W. Armstrong, B.L. Colborn, B. Anders, H. Brückmann, Jül-2203, Jülich, Germany, 1988.

(12) R.G. Alsmiller, J.M. Barnes and J.D. Drischler, Nucl. Instr. and Meth. A249 (1986) 455.

(13) H. Kluge and K. Weise, Rad. Protection Dosimetry 2 (1982) 85.

(14) P.A. Arnio, J. Lindgren, J. Ranft, A. Fasso and G.R. Stevenson, CERN Reports TIS-RP/168 (1986) and TIS-RP/190 (1987).

(15) J.M. Zazula, CERN (private communication).

(16) G.R. Stevenson, CERN Report TIS-RP/173 (1986).

(17) H. Dinter and K. Tesch, Rad. Protection Dosimetry 42 (1992) 5.

(18) K. Tesch, Rad. Protection Dosimetry 20 (1987) 169.

Target diam. (cm)	H per p (Sv)	$\frac{\text{H(0.15–22 MeV)}}{\text{H(22–400 MeV)}}$
0.2	$1.2 \cdot 10^{-14}$	2.7
2.	$5.9 \cdot 10^{-14}$	4.1
4.	$1.0 \cdot 10^{-13}$	4.9
10.	$1.9 \cdot 10^{-13}$	6.3

Tab. 1. The neutron dose equivalent per 100-GeV proton at a distance of 2 m from the target (see fig. 2) and the ratio of the two peaks in the neutron dose equivalent spectrum, as a function of target thickness.

Figure captions

Fig. 1. Attenuation of the dose equivalent H from an AmBe neutron source S. x calculations, * calculations corrected for detector response, • measurements (ref. 6). Attenuation formulae of ref. 6. (full line) and of ref. 7 (broken line).

Fig. 2. Geometries for calculating the plane source (full lines) and the attenuation of doses in labyrinths (example, broken lines).

Fig. 3. Neutron spectrum of the plane source (see fig. 2).

Fig. 4. Attenuation of the neutron dose equivalent H along straight access ways of different cross sections. Calculations (curves) and results of fitting formula equ. 2 (crosses).

Fig. 5. Attenuation of the neutron dose equivalent H in the second section of labyrinths with 5 different cross sections A, as a function of r_2 (upper right part) and as a function of $r_2/\sqrt{A}$ (lower left part).

Fig. 6. Neutron spectra in the second section of a labyrinth from the proton-induced plane source (full line) and from an AmBe neutron source (broken line).

Fig. 7. Comparison between the attenuation functions in the second and third section of a labyrinth and the corresponding attenuation curve for thermal neutrons.

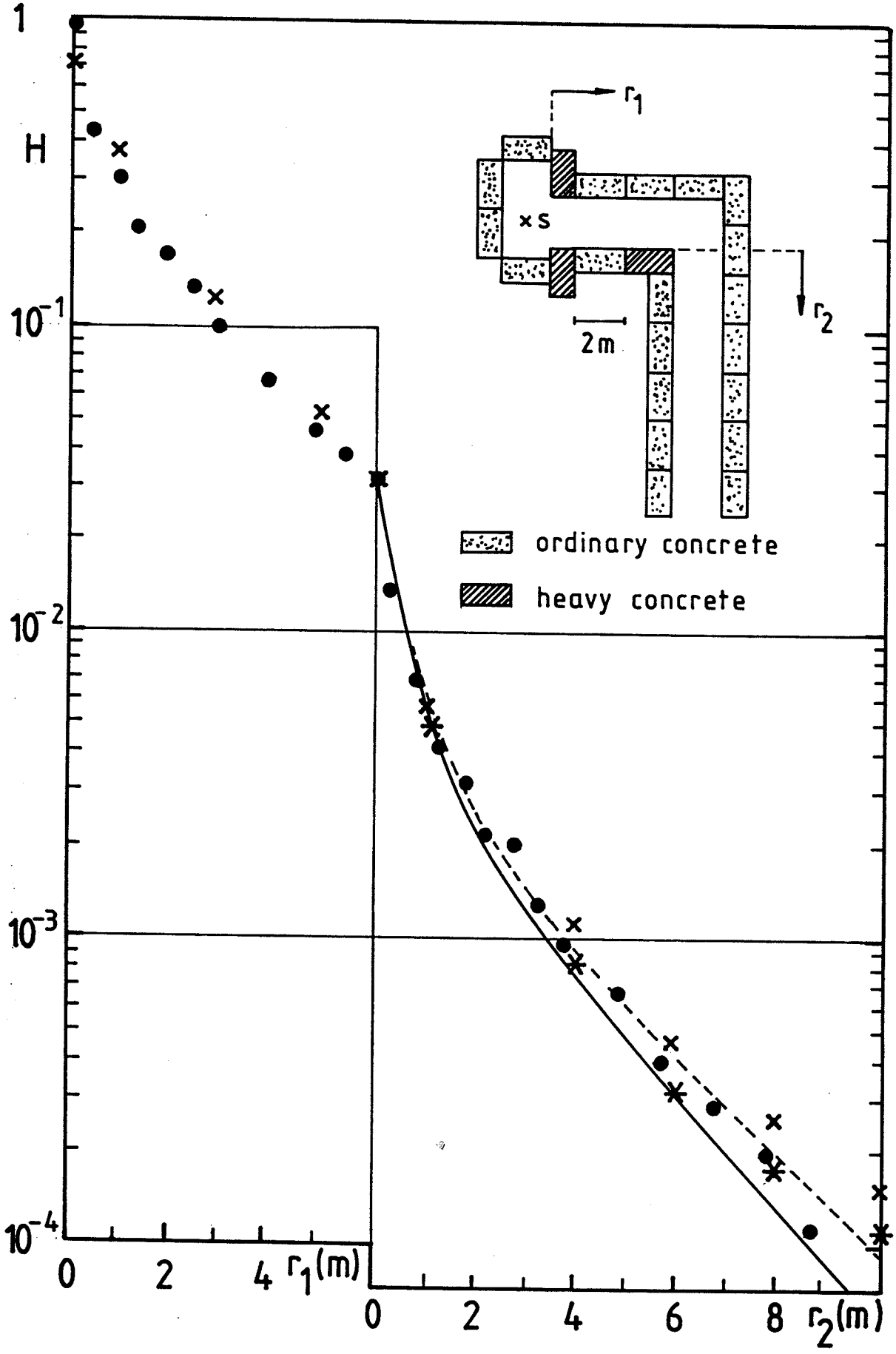
1
H
10^{-1}
10^{-2}
10^{-3}
10^{-4}
0
2
4
r_1(m)
0
2
4
6
8
r_2(m)
r_1
r_2
S
2m
ordinary concrete
heavy concrete

fig. 1

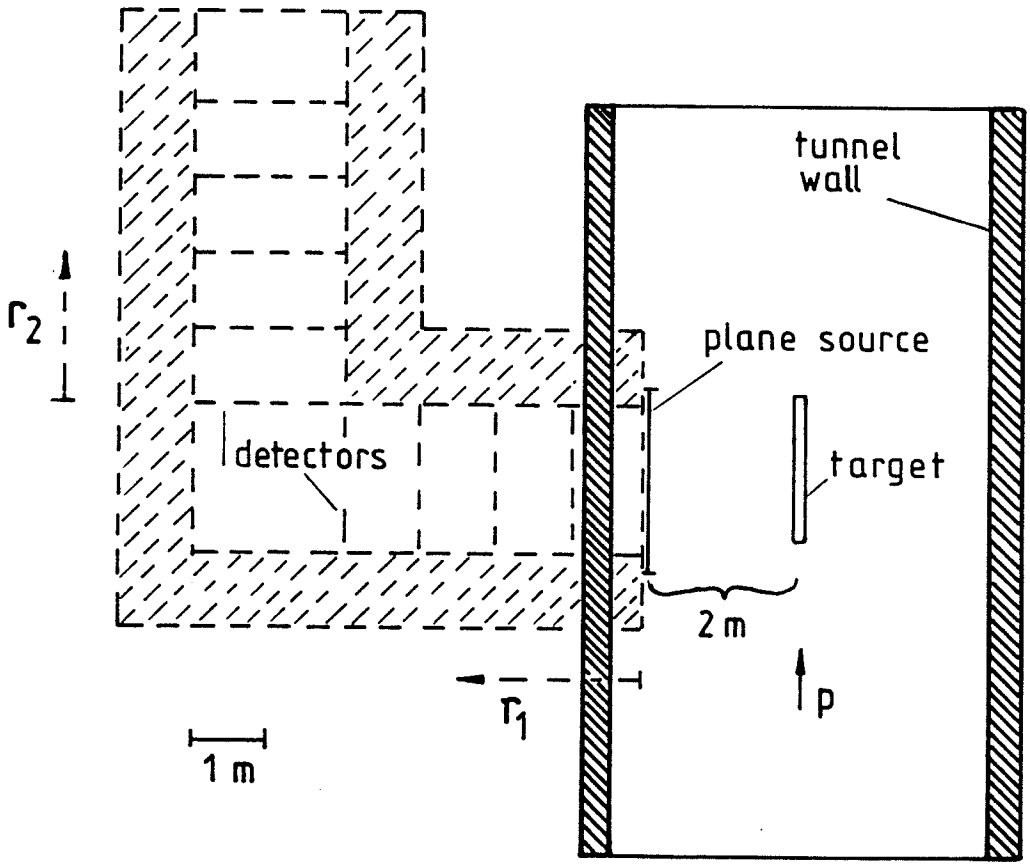

fig. 2

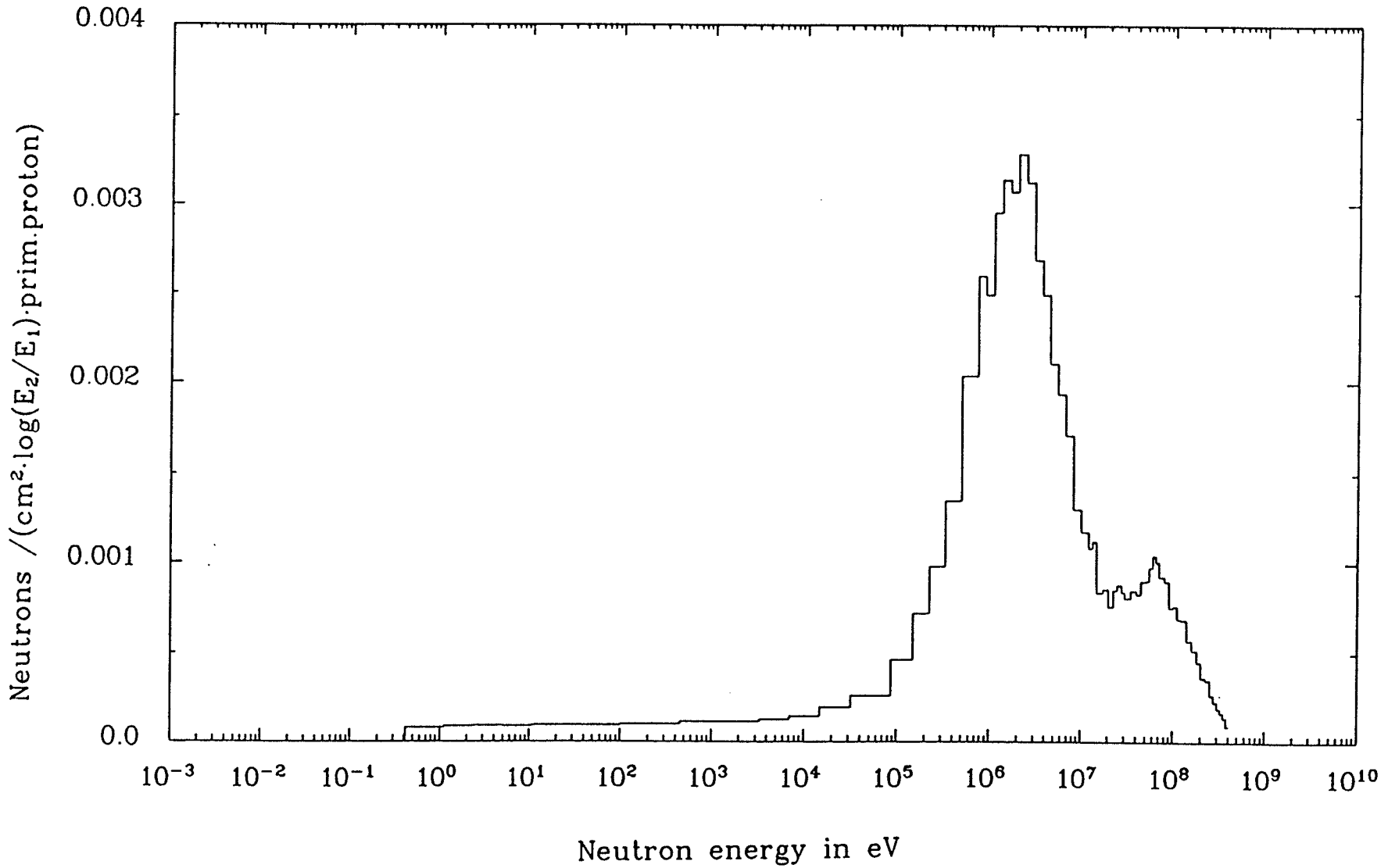
0.004
0.003
0.002
0.001
0.0
Neutrons /(cm².log(E₂/E₁)·prim.proton)
10⁻³ 10⁻² 10⁻¹ 10⁰ 10¹ 10² 10³ 10⁴ 10⁵ 10⁶ 10⁷ 10⁸ 10⁹ 10¹⁰
Neutron energy in eV

fig. 3

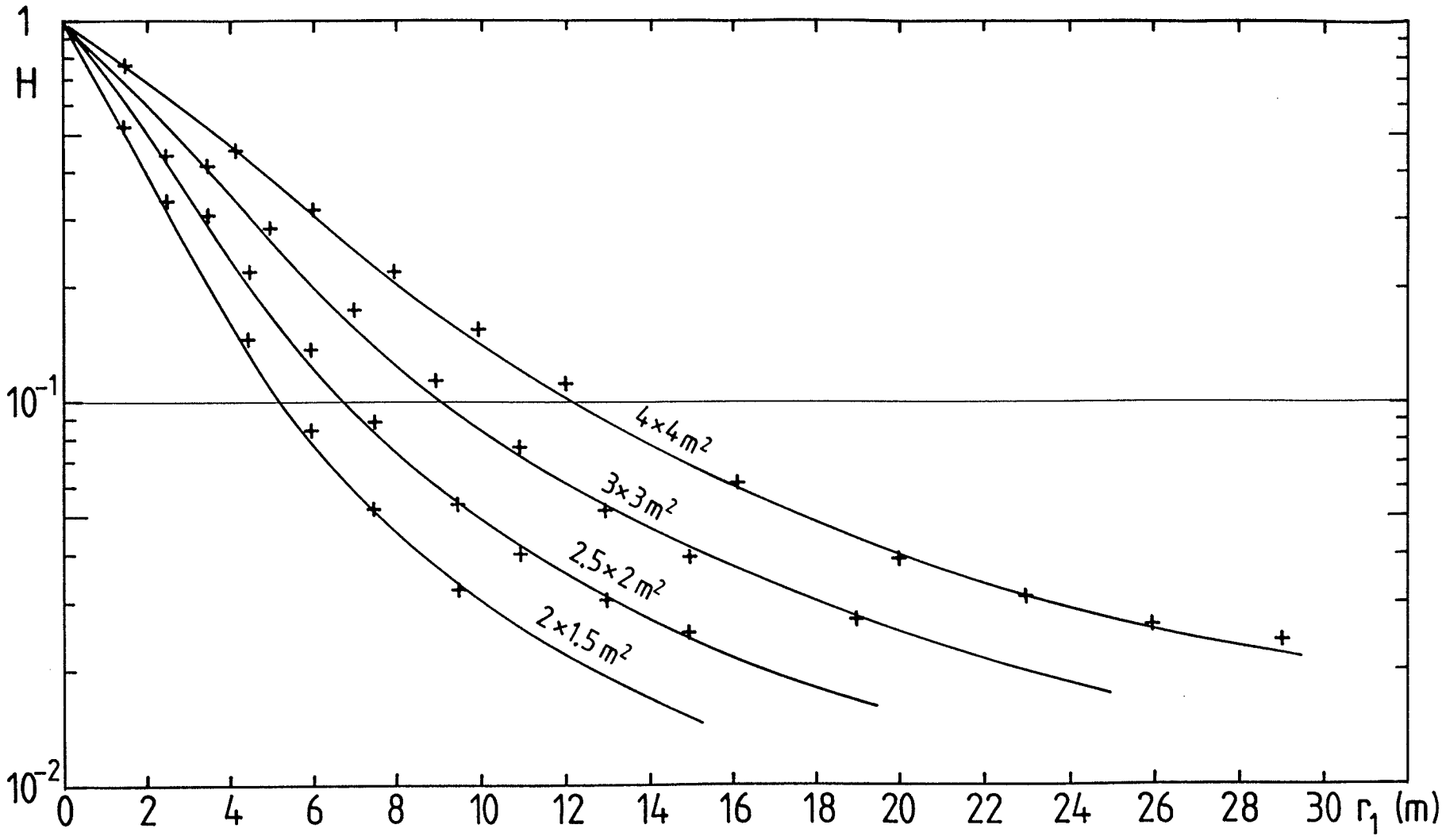
1
H
10^{-1}
10^{-2}
0
2
4
6
8
10
12
14
16
18
20
22
24
26
28
30
r_1 (m)
4×4m²
3×3m²
2.5×2m²
2×1.5m²

fig. 4

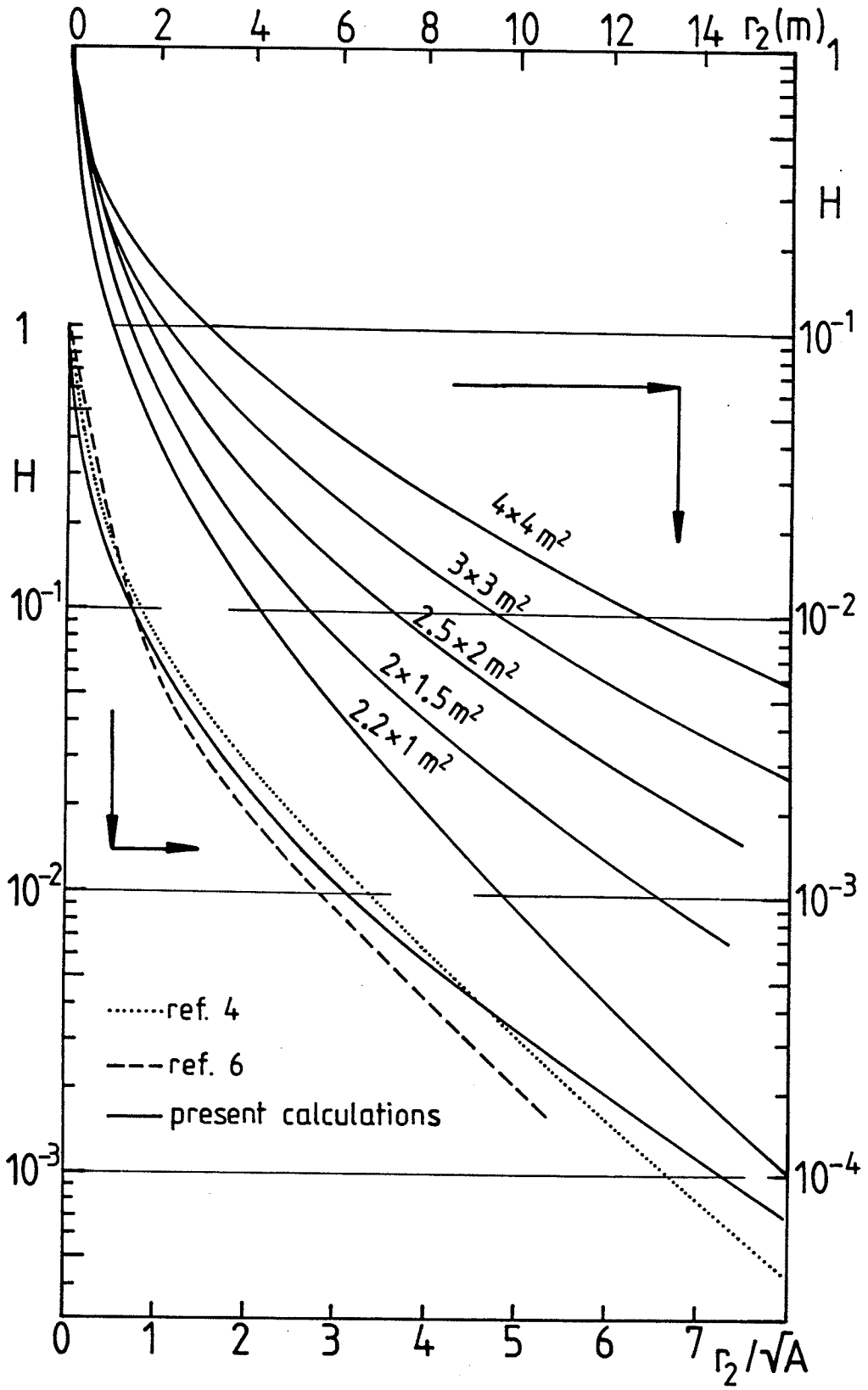
0 2 4 6 8 10 12 14 r2(m)
1
H
10-1
10-2
10-3
10-4
4×4 m²
3×3 m²
2.5×2 m²
2×1.5 m²
2.2×1 m²
ref. 4
ref. 6
present calculations
0 1 2 3 4 5 6 7 r2/√A

fig. 5

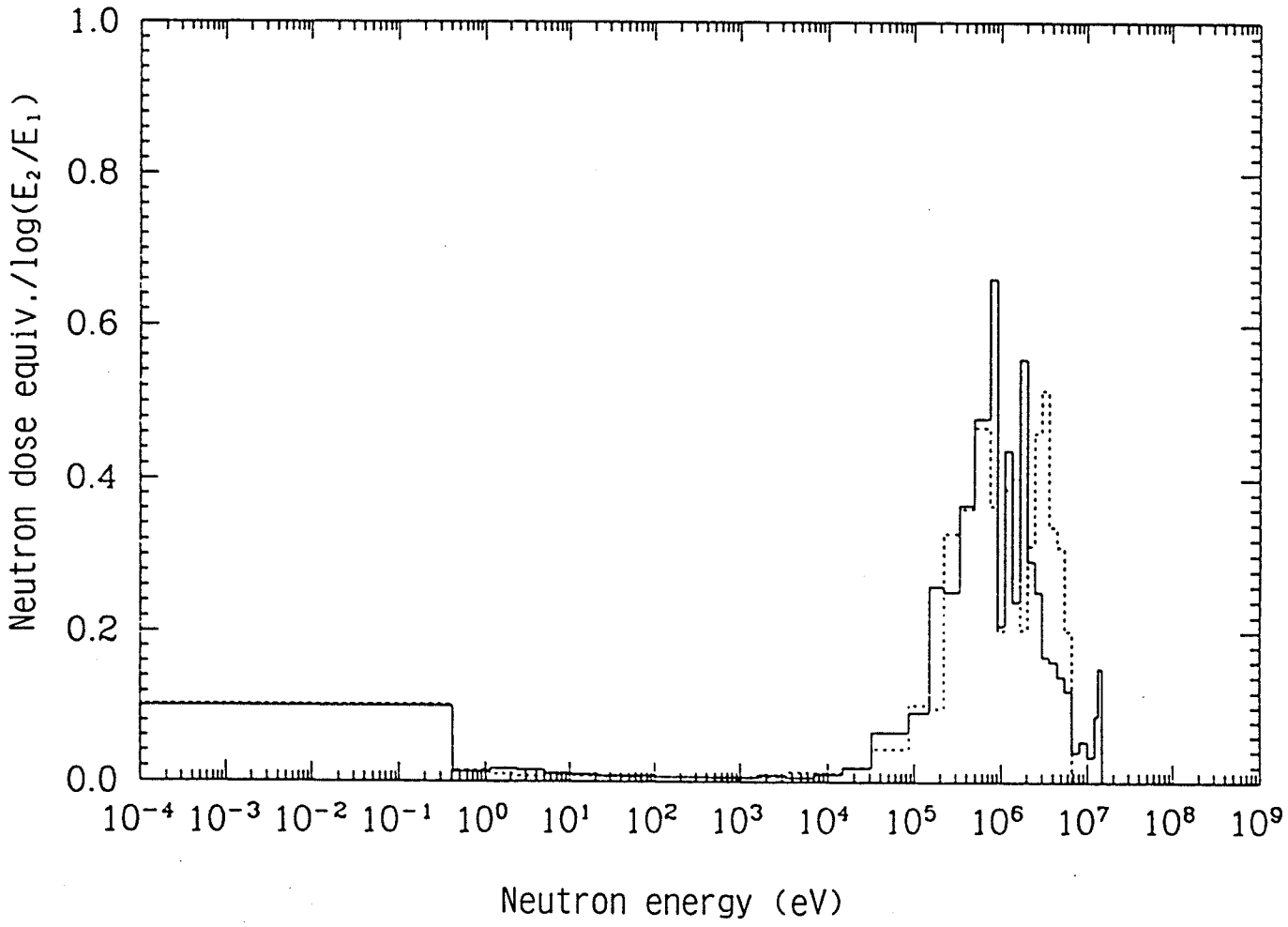
1.0
0.8
0.6
0.4
0.2
0.0
Neutron dose equiv./log(E2/E1)
10-4 10-3 10-2 10-1 100 101 102 103 104 105 106 107 108 109
Neutron energy (eV)

fig. 6

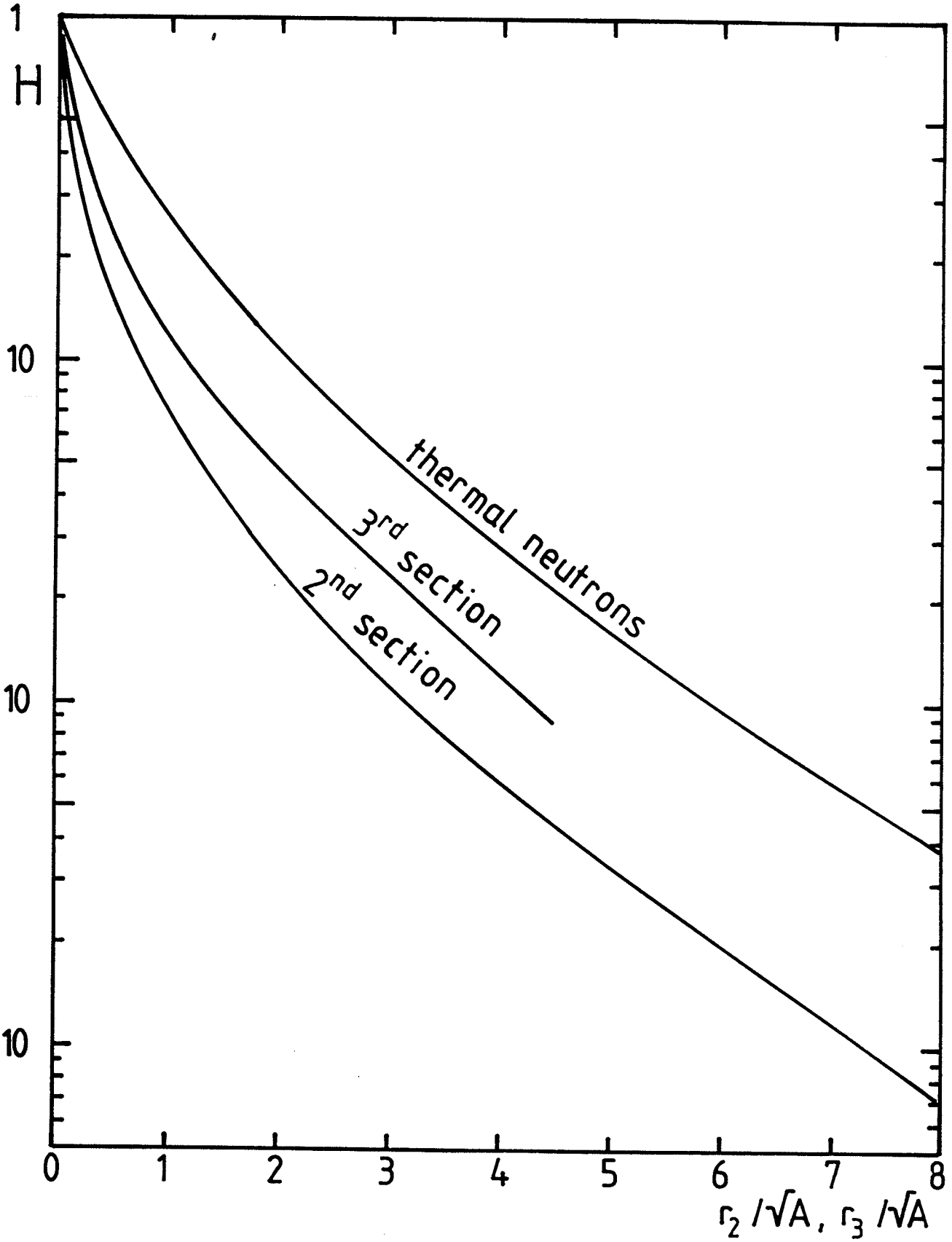
1
H
10
10
10
thermal neutrons
3rd section
2nd section
0
1
2
3
4
5
6
7
8
r2 /√A , r3 /√A

fig. 7